Electronic materials

CrossMark

Efficient red-emitting phosphor ScVO$_4$ doped with Bi^{3+} and Eu^{3+} for near-ultraviolet-activated solid-state lighting

Fengfeng Chi[1], Yanguang Qin[1], Fangfang Hu[1], Xiantao Wei[1,*], Yonghu Chen[1,*] (iD), Changkui Duan[1], and Min Yin[1]

[1] *Key Laboratory of Strongly-Coupled Quantum Matter Physics, Chinese Academy of Sciences, School of Physical Sciences, University of Science and Technology of China, No. 96 Jinzhai Road, Hefei, Anhui Province 230026, People's Republic of China*

ABSTRACT

In this paper, Bi^{3+}- and Eu^{3+}-co-doped ScVO$_4$ had been investigated as an alternative red-emitting phosphor under near-ultraviolet excitation. Structural and spectroscopic characterizations were carried out. The results show that the samples can efficiently absorb near-ultraviolet light and produce very bright red emission. In particular, the optimized sample shows much stronger emission intensity than the commercial phosphor Y$_2$O$_2$S: 5% Eu^{3+} in the excitation range of 365–395 nm, and can reach a strength 5.4 times of the latter under 385 nm excitation. It also has better CIE chromaticity coordinates. These suggest ScVO$_4$: Bi^{3+}, Eu^{3+} as a promising red-emitting phosphor for white light-emitting diodes based on near-ultraviolet light-emitting diode chips.

Introduction

Solid-state white light-emitting diodes (LEDs) developments have been blooming since the landmark achievement of bright-blue LEDs came out in the mid-1990s. A typical white LED, covering the broadband yellow-emitting phosphor YAG: Ce^{3+} on a blue LED chip, has been widely applied in many fields, owing to its superior properties such as high efficiency, energy-saving, friendly to the environment and long lifetime. Unfortunately, the major drawback of lacking red light component limits such white-lighting fixture to have a poor color rendering index (CRI, usually <75) and high correlated color temperature (CCT, 4000–8000 K) [1–7]. To generate a warm white light (CRI >80; CCT <4000 K), there is much room to improve. Many strategies have been proposed and that coating red–green–blue (RGB) tricolor phosphors on near-ultraviolet (NUV) LED chips (365–395 nm) is considered as one of the optimal [8].

In contrast to blue and green components, red-emitting phosphors still demand great attentions to enhance their performance [9]. Divalent Eu ion (Eu^{2+})-activated nitrides can give off very bright red light, which, however, is always quite far into deep red region where human eye is insensitive. Moreover, they could absorb visible light covering as far as the

red spectral scope thus may suffer from color change and lower luminous efficiency (efficiency of light conversion subject to the human eye sensitivity) [6, 10]. Trivalent Eu ion (Eu^{3+}) is considered as an ideal source of red light with excitation lines at NUV region. Traditional high-efficient red-emitting phosphors activated by Eu^{3+} ions such as Y_2O_2S: Eu^{3+} and YVO_4: Eu^{3+}, however, show a dramatic decrease in excitation efficiency in the NUV region and a tiny, narrow absorption around 395 nm, not suitable for NUV-activated white light applications. Therefore, host materials that can efficiently absorb NUV light and then transfer to red-emitting center is imperative.

For orthovanadates, the polarization of the oxygen ions resulting from the introduction of foreign ions in the host lattice influences the position of charge-transfer bands. By replacing Y^{3+} with trivalent cation with a smaller radius, such as Sc^{3+} and Lu^{3+}, the absorption band of $LnVO_4$ (Ln = Lu or Sc) doped with Eu^{3+} had a large red shift, which would be more significant upon introduction of Bi^{3+} ion [11, 12]. A sketch (Fig. 1) presents the energy absorption and transfer mechanism in $LnVO_4$: Bi^{3+}, Eu^{3+}. Besides the famous charge-transfer (CT) transition between O^{2-} and V^{5+} (O–V), the metal–metal CT transition between Bi^{3+} and V^{5+} is also taken into account in view of the 6s level of Bi^{3+} that lies above the highest filled 2p level of O^{2-} and the electron in the 6s level is apt to transfer to the empty 3d level of V^{5+}. The absorption band is accordingly extended to violet range upon introduction of Bi^{3+}. Moreover, the high energy levels of Eu^{3+} are embedded into the conduction band (V-3d states), so the energy transfer to Eu^{3+} could be highly efficient.

In this work, through a conventional high-temperature solid-state reaction, we synthesize samples of $ScVO_4$: Bi^{3+}, Eu^{3+} and optimize the doping proportion to achieve the best luminous efficiency. Under NUV light excitation, the obtained products show an excellent performance which will be discussed as follows.

Experimental

The samples of $ScVO_4$: Bi^{3+}, Eu^{3+} were synthesized through a conventional high-temperature solid-state reaction in air. The started materials were Sc_2O_3 (99.99%), Bi_2O_3 (AR), V_2O_5 (99.99%), Eu_2O_3 (99.99%). First, the raw materials were mixed according to a stoichiometric ratio and ground in an agate mortar. Then, the mixture was transferred into a ceramic crucible. The presintering step was performed at 750 °C for 4 h in a muffle furnace. After that, the samples were ground again and sintered at 1000 °C for 5 h. Finally, the obtained samples were ground to be powders for the subsequent measurements.

The XRD data were recorded via X-ray diffractometer (MAC Science Co. Ltd MXP18AHF), using nickel-filtered Cu K$_\alpha$ radiation ($\lambda = 1.5418$ Å) in the range of $2\theta = 10$–70°. The excitation and emission spectra were recorded with a Hitachi 850 fluorescence spectrophotometer using a 150-W xenon lamp as the excitation source. The decay curves were measured with a Tektronix TDS2024 digital storage oscilloscope under the excitation of 355 nm pulse laser yielded in a Q-switched flash-pumped Nd: YAG laser with the pulse duration of 10 ns.

Results and discussion

XRD characterization

The XRD patterns of the samples are shown in Fig. 2, along with the standard data of $ScVO_4$ (PDF-6-260). All the strong diffraction peaks agree well with the standard data, which belong to the zircon-type structure of space group $I4_1/amd$. Bi^{3+} and Eu^{3+} ions are supposed to occupy the Sc^{3+} sites, and because of larger ionic radii of Bi^{3+} and Eu^{3+} than Sc^{3+}, the peaks shift slightly to small angle with increasing the
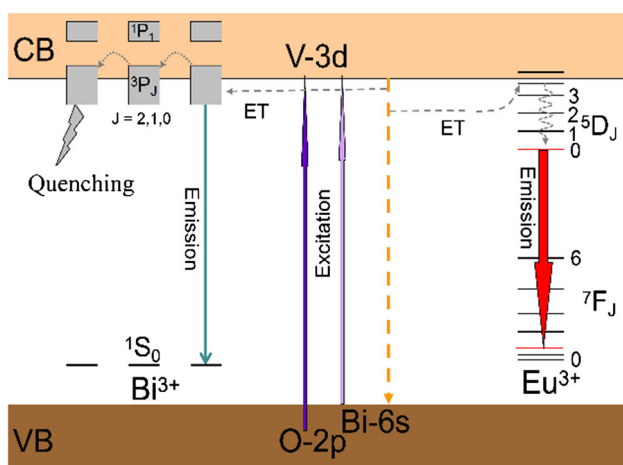

Figure 1 Sketch of probable energy absorption, transfer and relaxation processes in $ScVO_4$: Bi^{3+}, Eu^{3+}.
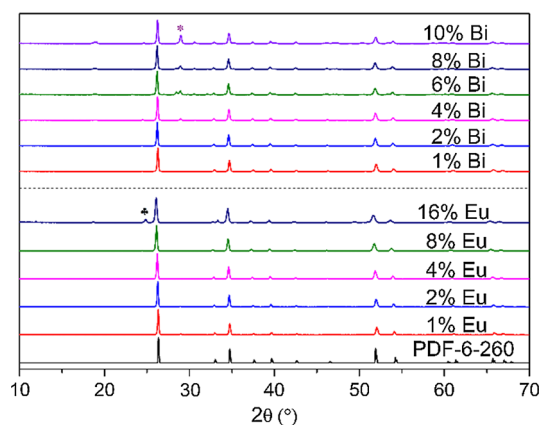
Figure 2 X-ray powder diffraction patterns of Eu^{3+}- and Bi^{3+}-co-doped $ScVO_4$ samples. For the patterns in the *upper part*, the concentration of Eu^{3+} is fixed at 4%, while for those in the *lower part*, the concentration of Bi^{3+} is fixed at 2%. PDF-6-260 is the standard data for $ScVO_4$.

doping proportion of Bi^{3+} or Eu^{3+}. It is noteworthy that two tiny impurity peaks at 29° and 25° emerge when the doping increases to a relatively heavy level, which are, respectively, ascribed to the main diffraction peak of $BiVO_4$ and $EuVO_4$. Such impurity will shrink the expected concentration of the concerned ion in the final product, suggesting heavy doping in this host is unsuitable.

Luminescent properties

Figure 3 shows the luminescent properties of $ScVO_4$ doped with Eu^{3+} and Bi^{3+} samples, composed of excitation spectra (a) monitored the emission at 616 nm (Eu^{3+}, $^5D_0 \rightarrow {}^7F_2$) and emission spectra under 395 nm excitation for samples with different doping concentrations of Bi^{3+} (b) and Eu^{3+} (c). In the excitation spectra, besides the weak narrow peaks from 450 to 550 nm corresponding to the Eu^{3+} 4f–4f transitions, there are intense broadbands covering from 200 to 430 nm which are attributed to the overlap of O–Eu, O–V and Bi–V CT transitions, as proposed earlier [11]. It is of significance that upon introduction of Bi^{3+} ions in the host a striking shoulder bursts from 350 to 430 nm attaching to the dominant O–V CT transition centered at 326 nm. This shoulder has been identified as the Bi–V metal–metal CT transition, ascribed to electron transfer from Bi-6s state to V-3d state [11]. It should be noted that the charge-transfer transition is allowed by the spin and parity selection rules, which is responsible for the efficient absorption of NUV light, and here

overwhelmingly outshines the parity-forbidden intra-4f transition of Eu^{3+}. It should also be worthy of mention that for many Eu^{3+}-activated red-emitting materials, the near-ultraviolet absorption around 395 nm is usually attributed to the transition of $^7F_0 \rightarrow {}^5L_6$, which is always weak unless the doping is heavy. Moreover, shielded by the filled $5s^2$ and $5p^6$ shell, the intra-4f transition is generally narrow and sharp, leading the excitation efficiency to be vulnerable to the tiny emission wavelength shift of the NUV LED chip at various temperatures. Fortunately, owing to the sensitization of Bi^{3+}, the current material $ScVO_4$: Bi^{3+}, Eu^{3+} has shown a broad excitation band covering NUV, indicating it a promising candidate for excellent NUV-excited red-emitting phosphor.

On the other hand, the presence of energy transfer from CT band to Eu^{3+} ions can be verified by the observation of the charge-transfer band in the excitation spectra of Eu^{3+} ions. When the doping concentration of Bi^{3+} increases, the O–V CT band decreases monotonously, while the Bi–V CT band rises to the maximum until the doping concentration of Bi^{3+} reaches 2%. As elucidated in Fig. 1, two relaxation paths are considered for the excitation energy in this material: One is quenching in Bi^{3+} ions, and the other is being emitted by Eu^{3+} ions. The decline of O–V CT band in the Eu^{3+} excitation spectra is ascribed to the increase in the energy transfer from O–V CT band to Bi^{3+}, and part of the excitation energy would subsequently be quenched in Bi^{3+} ions. The excitation energy transferred to Eu^{3+} ions is thus reduced, resulting in a decline of O–V CT band in the excitation spectra.

The rising of Bi–V band is owing to the increase in the absorption of Bi–V CT band and the energy transfer possibility to Eu^{3+} ions, resulting in a stronger Eu^{3+} emission, i.e., a higher Bi–V CT band. However, when the doping concentration of Bi^{3+} exceeded 2%, energy transfer from Bi–V CT band to Eu^{3+} ions would be reduced due to the fast increase in nonradiative relaxation in Bi^{3+} ions, leading to the suppression of Bi–V CT band in the excitation spectra. So, it is conclusive that the excitation energy prefers to quench in Bi^{3+} ions rather than transfer to Eu^{3+} in high doping concentration of Bi^{3+}. In other words, the doping of Bi^{3+} should not be high in this host material for good luminescence. A similar phenomenon was also reported in Ref. 13 for Bi^{3+} singly doped $ScVO_4$ samples. Only in the case of very low
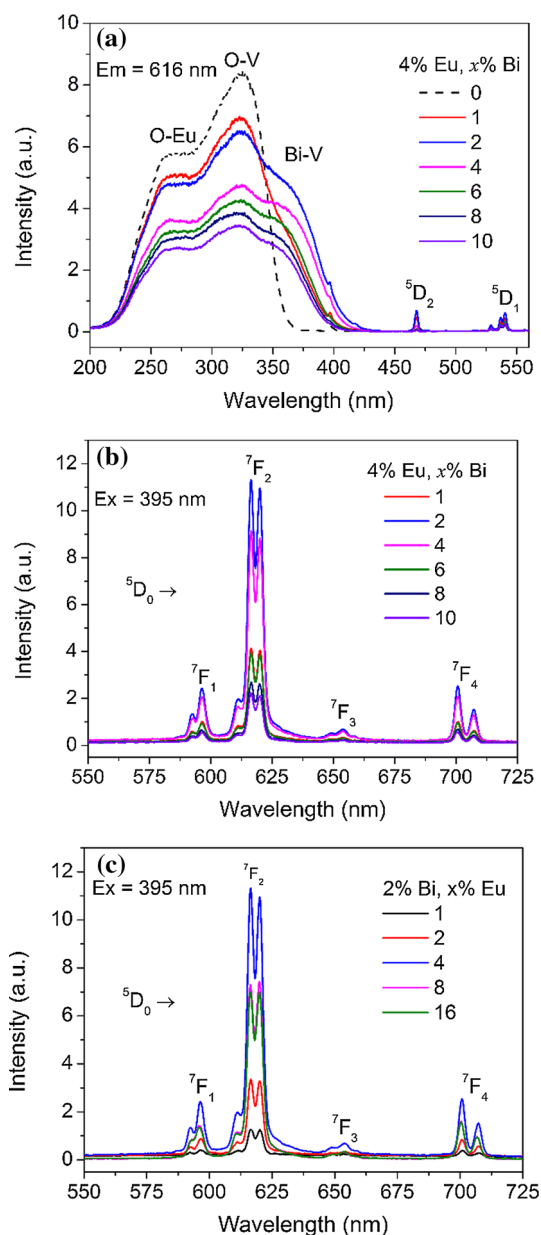
Figure 3 a Excitation spectra of $ScVO_4$: $x\%$ Bi^{3+}, 4% Eu^{3+} ($x = 0, 1, 2, 4, 6, 8, 10$) by monitoring 616 nm from $^5D_0 \rightarrow \,^7F_2$ transition of Eu^{3+}. **b** Corresponding emission spectra excited at 395 nm. **c** Emission spectra of $ScVO_4$: 2% Bi^{3+}, $x\%$ Eu^{3+} ($x = 1, 2, 4, 8, 16$) under 395 nm excitation.

Bi^{3+} doping concentration (usually lower than 2 or 1%), exciting into O–V CT band could give off the Bi^{3+} broadband $^3P_1 \rightarrow \,^1S_0$ emission centered at 635 nm. This emission drops quickly with increasing the doping concentration of Bi^{3+} because the nonradiative relaxation would dominate [13].

Under 395 nm light excitation, the samples doped with Eu^{3+} emit very bright red light, corresponding to $^5D_0 \rightarrow \,^7F_2$ transition of Eu^{3+}. As seen in Fig. 3b, the Eu^{3+} electric dipole transition $^5D_0 \rightarrow \,^7F_2$ is much stronger than magnetic dipole transition $^5D_0 \rightarrow \,^7F_1$. It is because the Sc^{3+} site in $ScVO_4$ has very large deviation from centrosymmetry. Such site surrounding is desired for Eu^{3+}-activated red-emitting phosphor to gain a suitable color rendering index. The samples doped with 2 and 4% Bi^{3+} yield apparently the stronger red emission, submerged by a very week broadband. In view of the V–O CT band emission has a quenching temperature far below room temperature and always locates around 465 nm, the week bands mentioned above are accordingly considered to originate from Bi^{3+} $^3P_1 \rightarrow \,^1S_0$ transition centered at 635 nm [13], and here is too weak to significantly alter the energy distribution of emission. So, it can be concluded that the excitation energy could be efficiently transferred to Eu^{3+} when the doping concentration of Bi^{3+} is below 2%. For those with higher doping concentration, the quenching in Bi^{3+} ions grows rapidly to dominate the majority of the relaxation, resulting in much weaker Eu^{3+} emission. This is in accordance with the situation in excitation spectra.

The dependence of integrated emission intensity on the doping concentrations of Eu^{3+} or Bi^{3+} is plotted in Fig. 4a, b, respectively. The ideal doping level of Eu^{3+} is 4%. As shown in Fig. 4c, the decay lifetimes of $^5D_0 \rightarrow \,^7F_2$ emission of Eu^{3+} at 616 nm for
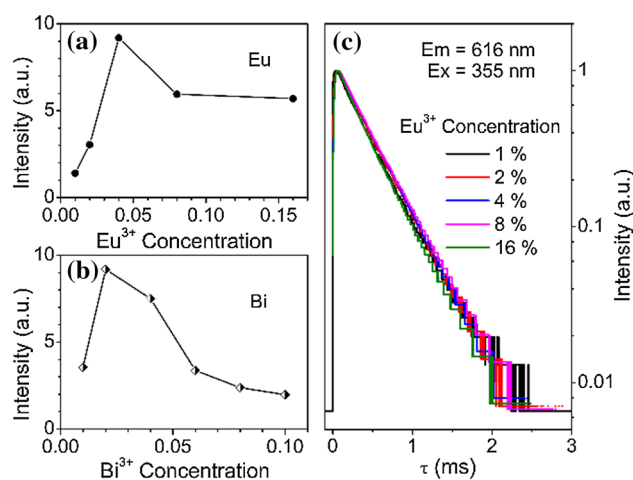

Figure 4 Dependence of integrated emission intensity on concentrations of Eu^{3+} (Bi^{3+} concentration being 2%) (**a**) and Bi^{3+} (Eu^{3+} concentration being 4%) (**b**) under the excitation of 395 nm. Decay curves of Eu^{3+} $^5D_0 \rightarrow \,^7F_2$ transition at 616 nm of $ScVO_4$ doped with 2% Bi^{3+} and a series of Eu^{3+} concentrations (**c**).

2% Bi^{3+}-doped $ScVO_4$ samples are almost invariant for different Eu^{3+} concentrations. The above results indicate that there is no back energy transferring from Eu^{3+} to Bi^{3+}. Therefore, the Eu^{3+} luminescence quenching in high doping concentration may be due to the formation of slight $EuVO_4$, as shown in the XRD patterns.

A comparison on luminescence performance between the optimized $ScVO_4$: Bi^{3+}, Eu^{3+} and the commercial red-emitting phosphor Y_2O_2S: 5% Eu^{3+} is shown in Fig. 5. Distinct characteristics can be seen in both excitation and emission spectra. In the scope from 360 to 410 nm in the excitation spectra, obviously the optimized sample $ScVO_4$: 2% Bi^{3+}, 4% Eu^{3+} with the contribution of Bi–V CT band shows more efficient excitation than Y_2O_2S: 5% Eu^{3+}. Accordingly, with NUV light excitation, $ScVO_4$: 2% Bi^{3+}, 4% Eu^{3+} shows more bright red emission than Y_2O_2S: 5%Eu^{3+} does. Concretely speaking, the former yields red emissions 4.6, 5.4, 3.1 and 1.7 times of the latter, respectively, under 395, 385, 375 and 365 nm

excitations. Moreover, the main emission peak of $ScVO_4$: 2%Bi^{3+}, 4%Eu^{3+} is located at 616 nm, which is an ideal peak position to provide good color rendering [7], whereas Y_2O_2S: 5% Eu^{3+} gives off a relatively deep red emission mainly at 627 nm. Besides, the CIE chromaticity coordinates for $ScVO_4$: 2% Bi^{3+}, 4% Eu^{3+} are calculated to be (0.65, 0.35), closer to the National Television System Committee standard value (0.67, 0.33) for red-emitting phosphor, compared with those of Y_2O_2S: 5% Eu^{3+} (0.64, 0.36). These results propose $ScVO_4$: 2% Bi^{3+}, 4% Eu^{3+} to be a very competitive candidate for red component in tricolor-based white LEDs.

Conclusion

In summary, a series of $ScVO_4$: Bi^{3+}, Eu^{3+} samples were successfully synthesized, and their luminescent properties were investigated in detail to achieve the best luminous efficiency. The experimental results show that the samples exhibit very efficient excitation in NUV range and can be excited even at 430 nm. All samples show the characteristic red emission of Eu^{3+} at 616 nm corresponding to $^5D_0 \rightarrow {}^7F_2$ transition. And the optimized one produces an emission intensity 5.4 times of the commercial phosphor Y_2O_2S: 5%Eu^{3+} under 385 nm excitation. Moreover, it also has a better CIE chromaticity coordinates than the latter, closer to the National Television System Committee standard value for red-emitting phosphor. These results suggest that $ScVO_4$: Bi^{3+}, Eu^{3+} is promising for NUV-excited white LEDs in illumination applications.
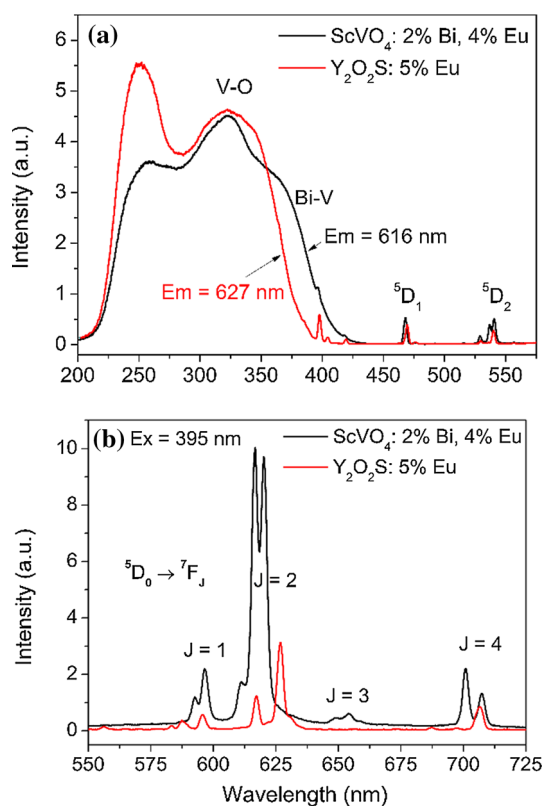
Figure 5 Comparison of **a** excitation and **b** emission spectra between $ScVO_4$: 2% Bi^{3+}, 4% Eu^{3+} (*black curve*) and Y_2O_2S: 5% Eu^{3+} (*red curve*).

Compliance with ethical standards

Conflict of interest The authors declare that they have no conflict of interest.

References

[1] Pust P, Schmidt PJ, Schnick W (2015) A revolution in lighting. Nat Mater 14:454–458

[2] George NC, Denault KA, Seshadri R (2013) Phosphors for solid-state white lighting. Annu Rev Mater Res 43:481–501

[3] Sheu JK, Chen FB, Wang YC, Chang CC, Huang SH, Liu CN, Lee ML (2015) Warm-white light-emitting diode with high color rendering index fabricated by combining trichromatic InGaN emitter with single red phosphor. Opt Express 23:A232–A239

[4] Ye S, Xiao F, Pan YX, Ma YY, Zhang QY (2010) Phosphors in phosphor-converted white light-emitting diodes recent advances in materials, techniques and properties. Mat Sci Eng R 71:1–34

[5] Chen L, Lin CC, Yeh CW, Liu RS (2010) Light converting inorganic phosphors for white light-emitting diodes. Materials 3:2172–2195

[6] Pust P, Weiler V, Hecht C, Tucks A, Wochnik AS, Henss AK, Wiechert D, Scheu C, Schmidt PJ, Schnick W (2014) Narrow-band red-emitting $Sr[LiAl_3N_4]$: Eu^{2+} as a next-generation LED-phosphor material. Nat Mater 13:891–896

[7] Coltrin ME, Armstrong AM, Brener I, Chow WW, Crawford MH, Fischer AJ, Kelley DF, Koleske DD, Lauhon LJ, Martin JE, Nyman M, Schubert EF, Shea-Rowher LE, Subramania G, Tsao JY, Wang GT, Wierer JJ, Wright JB (2014) Energy frontier research center for solid-state lighting science: exploring new materials architectures and light emission phenomena. J Phys Chem C 118:13330–13345

[8] Deng KM, Gong T, Chen YH, Duan CK, Yin M (2011) Efficient red-emitting phosphor for near-ultraviolet-based solid-state lighting. Opt Lett 36:4470–4472

[9] Zhu HM, Lin CC, Luo WQ, Shu ST, Liu ZG, Liu YS, Kong JT, Ma E, Cao YG, Liu RS, Chen XY (2014) Highly efficient non-rare-earth red emitting phosphor for warm white light-emitting diodes. Nat Commun 5:4312-1–4312-10

[10] Pust P, Wochnik AS, Baumann E, Schmidt PJ, Wiechert D, Scheu C, Schnick W (2014) $Ca[LiAl_3N_4]$:Eu^{2+}-a narrow-band red-emitting nitridolithoaluminate. Chem Mater 26:3544–3549

[11] Wei XT, Wen J, Li S, Huang S, Cheng J, Chen YH, Duan CK, Yin M (2014) Red-shift of vanadate band-gap by cation substitution for application in phosphor-converted white light-emitting diodes. Appl Phys Lett 104:181904-1–181904-4

[12] Blasse G, Bril A (1969) Luminescence of phosphors based on host lattices ABO_4 (A is Sc, In; B is P, V, Nb). J Chem Phys 50:2974–2980

[13] Kang FW, Yang XB, Peng MY, Wondraczek L, Ma ZJ, Zhang QY, Qiu JR (2014) Red photoluminescence from Bi^{3+} and the influence of the oxygen-vacancy perturbation in $ScVO_4$: a combined experimental and theoretical study. J Phys Chem C 118:7515–7522